

Quantum coherent  $\pi$ -electron rotations in a non-planar chiral molecule induced by using a linearly polarized UV laser pulse

This content has been downloaded from IOPscience. Please scroll down to see the full text.

2015 J. Phys.: Conf. Ser. 627 012020

(<http://iopscience.iop.org/1742-6596/627/1/012020>)

View [the table of contents for this issue](#), or go to the [journal homepage](#) for more

Download details:

IP Address: 108.61.250.221

This content was downloaded on 26/06/2016 at 16:27

Please note that [terms and conditions apply](#).

# Quantum coherent $\pi$ -electron rotations in a non-planar chiral molecule induced by using a linearly polarized UV laser pulse

Hirobumi Mineo<sup>1</sup> and Yuichi Fujimura<sup>2</sup>

<sup>1</sup>Institute of atomic and molecular science, No.1 Section 4, Roosevelt road, Taipei, 115, Taiwan

<sup>2</sup>Department of Applied Chemistry, Institute of Molecular Science and Center for Interdisciplinary Molecular Science, National Chiao Tung University, Hsinchu 30010, Taiwan

E-mail: mineo@gate.sinica.edu.tw

**Abstract.** We propose an ultrafast quantum switching method of  $\pi$ -electron rotations, which are switched among four rotational patterns in a nonplanar chiral aromatic molecule (*P*)-2,2'-biphenol and perform the sequential switching among four rotational patterns which are performed by the overlapped pump-dump laser pulses. Coherent  $\pi$ -electron dynamics are generated by applying the linearly polarized UV pulse laser to create a pair of coherent quasi-degenerated excited states. We also plot the time-dependent  $\pi$ -electron ring current, and discussed ring current transfer between two aromatic rings.

## 1. Introduction

Recently organic electronics and devices have been actively studied [1-8] because of its potential usefulness. Particularly,  $\pi$ -electron dynamics in aromatic ring molecules are focused very much since  $\pi$ -electron shows high reactivity. The quantum simulations of  $\pi$ -electron ring current were performed in a higher symmetric planar molecules, Mg-porphyrin [9, 10]. Here the degenerated electronic states are excited by using the circularly polarized UV laser pulses. The rotational direction of the resultant "incoherent"  $\pi$ -electron ring current depends on whether the right or left circularly polarized laser pulse is applied, and the current is unidirectional. On the other hand the linearly polarized UV laser pulses can create a "coherent"  $\pi$ -electron ring current in a chiral aromatic molecule with lower symmetry. Kanno et. al. carried out numerical simulations of the  $\pi$ -electron rotation for 2,5-dichloro[n](3,6) pyrazinophane [11, 12], which is a planar chiral aromatic molecule. The rotational direction of  $\pi$ -electron ring current is determined by whether the superposition of quasi-degenerate coherent states excited by linearly polarized UV laser pulse is in-phase or out-phase. The results of numerical simulation indicates that the chiral aromatic molecule can be a candidate of the ultrafast switching device.

We have also studied coherent  $\pi$ -electron dynamics of a nonplanar chiral aromatic molecule (*P*)-2,2'-biphenol [13, 14]. This is a nonplanar chiral aromatic molecule with axial chirality, which has two aromatic rings (called *L* and *R* hereafter) linked through a single chemical bridge bond. We have classified four possible rotational patterns of  $\pi$ -electron rotations [13, 14] as CC, AC, CA, and AA



where C (A) represents clockwise (anticlockwise) rotational direction. Because of the nonplanar structure of (*P*)-2,2'-biphenol, the resultant  $\pi$ -electron rotation and angular momentum are two dimensional. This indicates that nonplanar chiral aromatic molecules like (*P*)-2,2'-biphenol may serve as a two-dimensional ultrafast switching device. For more effective quantum control of the ultrafast sequential switching among the above four rotational patterns, the overlapped pump and dump pulses with a properly selected relative phase and a laser polarization direction are necessary in addition to the time delay between pump and dump pulses.

The paper is organized as follows. In section 2 we mention an optimized geometry and electronic excited states of (*P*)-2,2'-biphenol, and in section 3 the four directional patterns of the  $\pi$ -electron rotations and angular momentum on each ring *L* and *R* are shown. In section 4 we plot time-dependent behaviors of  $\pi$ -electron ring currents on both aromatic rings and a bridge current between two rings, and demonstrate an ultrafast two-dimensional quantum switching of  $\pi$ -electron angular momentum in addition. In section 5 we summarize and conclude this paper.

## 2. Optimized geometry and electronic excited states of (*P*)-2,2'-biphenol

Here we consider a (*P*)-2,2'-biphenol, which is a simple, and a real nonplanar chiral aromatic molecule with two covalently bonded aromatic rings. The ground state geometry of (*P*)-2,2'-biphenol was optimized by using the DFT B3LYP level of theory in the GAUSSIAN09 program. The energy levels of the electronic excited states were calculated at the optimized ground state geometry by the TDDFT B3LYP level of theory. The 6-31G+(d,p) basis sets were used in our calculations. For generation of coherent angular momentum and ring current of (*P*)-2,2'-biphenol, we focus on the three optically allowed excited states (*a*, *b*<sub>1</sub> and *b*<sub>2</sub>). The electronic excited energies at the *a*, *b*<sub>1</sub> and *b*<sub>2</sub> states, which were calculated at the optimized ground state geometry using the TD-DFT B3LYP level of theory are 6.67, 6.78, and 6.84 eV, respectively. The transition dipole moments are shown in Fig. 1. The transition dipole moment from the ground state to excited state *a* (*A*),  $\vec{\mu}_{ga} (= (0, 0, -0.77))$  [a.u.], is parallel to the *Z*-axis, and the others,  $\vec{\mu}_{gb1} (= (0.08, 1.93, 0))$  and  $\vec{\mu}_{gb2} (= (1.24, -0.34, 0))$  [a.u.], are nearly orthogonal to each other in the *XY*-plane as shown in Fig. 1.

Coherent two electronic excited states (*a* ± *b*<sub>1</sub>), (*a* ± *b*<sub>2</sub>) and (*b*<sub>1</sub> ± *b*<sub>2</sub>) are generated by applying a UV laser pulse with a properly selected polarization direction. Here ( $\alpha + \beta$ ) ( $\alpha - \beta$ ) represents a phase between two electronic excited states is in-phase (out-phase). For example, for (*a* ± *b*<sub>2</sub>) electronic coherence, the condition for a linearly polarized UV laser pulse with polarization vector  $\vec{e}_{ab2}^{(\pm)}$  is given as  $\vec{\mu}_{ga} \bullet \vec{e}_{ab2}^{(\pm)} = \pm \vec{\mu}_{gb2} \bullet \vec{e}_{ab2}^{(\pm)}$ , and  $\vec{\mu}_{gb1} \bullet \vec{e}_{ab2}^{(\pm)} = 0$ .

Thus, even laser pulse overlaps with an *a*, *b*<sub>1</sub> and *b*<sub>2</sub>, (*a* + *b*<sub>2</sub>) or (*a* - *b*<sub>2</sub>) electronic coherent state can be selectively generated.

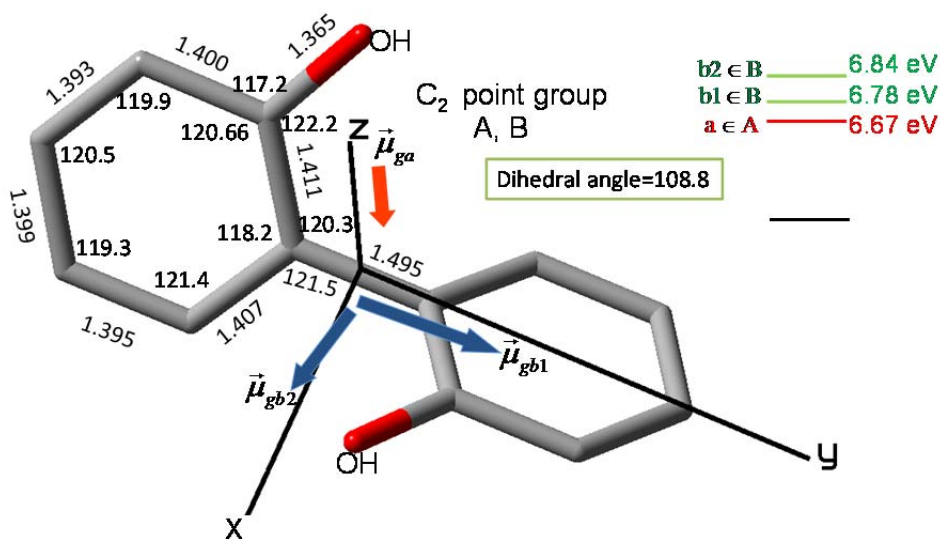


Figure 1. Geometrical structure of (*P*)-2,2'-biphenol with transition dipole moments between the ground state and three electronic excited states *a*, *b1* and *b2*. The unit of bond lengths is in angstrom ( $=10^{-10}$  m).

### 3. Methods

The initial directional patterns of  $\pi$ -electron rotations on each ring *L* and *R* are schematically depicted in Fig. 2. Here in the upper figure the selective electronic excited states with in- or out- phase are initially prepared by the UV laser pulse with the polarization direction  $\vec{e}_{ab1}^{(\pm)}$ ,  $\vec{e}_{ab2}^{(\pm)}$  and  $\vec{e}_{bib2}^{(\pm)}$ . From Fig. 2 in the upper it is observed that in the cases (i) and (ii) in which a superposition of same irreducible representations:  $(b_1 \pm b_2)$ ,  $\pi$ -electron rotations on each ring *L* and *R* oscillate in the same direction, whereas the bridge bond current is permanently zero. Whereas in other cases ring currents on each ring *L* and *R* oscillate in the opposite direction, as a characteristic feature a bond current between two rings *L* and *R* is generated.

Lower figure of Fig. 2 shows the resultant angular momentum  $\vec{l} = \vec{l}_L + \vec{l}_R$  corresponding to each initial directional pattern of ring currents respectively. The  $\pi$ -electron angular momentum  $\vec{l}_L$  ( $\vec{l}_R$ ) is perpendicular to the *L* (*R*) phenol ring, and in the cases (i) and (ii), i.e., in which a superposition of  $(b_1 \pm b_2)$ , the resultant total angular momentum (denoted as  $l_z$ ) is parallel to the Z axis, whereas in other cases in which a superposition of different irreducible representations:  $(a \pm b_1)$  or  $(a \pm b_2)$ , the resultant total angular momentum (denoted as  $l_x$ ) is parallel to the X axis, in the XZ plane.

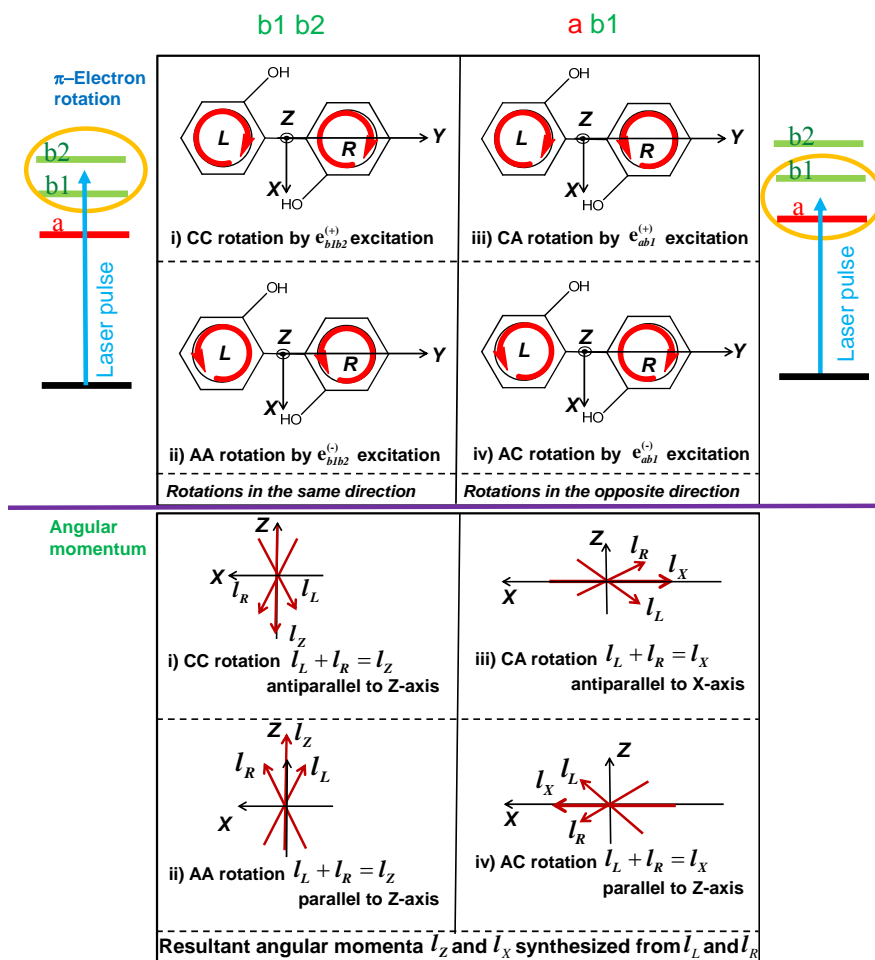


Figure 2. The initial directional patterns of  $\pi$ -electron rotations on each ring  $L$  and  $R$  induced by selective coherent electronic excited states  $(a \pm b_1)$ ,  $(a \pm b_2)$  and  $(b_1 \pm b_2)$  are shown in the upper figure. For example, CA rotation means directions of  $\pi$ -electron rotations on  $L$  and  $R$  are clockwise and anticlockwise respectively. (b) Resultant angular momentum  $l_x$  and  $l_z$  corresponding to each pattern of  $\pi$ -electron rotations are plotted respectively.  $l_L$  ( $l_R$ ) denotes the angular momentum created on the  $L$  ( $R$ ) ring.

#### 4. Results and discussions

Here we first show the results of the  $\pi$ -electron ring current generated on the (*P*)-2,2' biphenol, and demonstrate two-dimensional ultrafast quantum switching of the angular momentum.

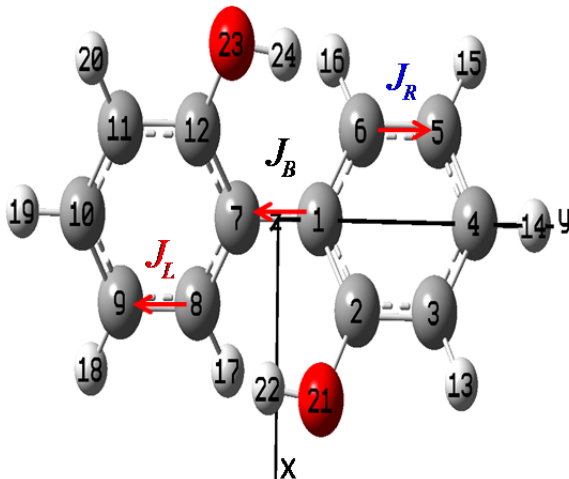
In Fig. 3(a) directions of the ring current  $J_L$  ( $J_R$ ) on  $L$  ( $R$ ) phenol ring, and the bridge bond current are defined. In figure 3(b) we shine the  $\pi$ -pulse gaussian-shaped LP laser pulse with the amplitude 1.2 GV/m and pulse duration 64 fs. Here polarization direction of the laser pulse is chosen as in-phase direction to coherently excite to quasi-degenerate electronic excited states  $b_1$  and  $b_2$ . It is observed that ring currents  $J_L$  and  $J_R$  oscillate in the same phase, whereas the bridge bond current  $J_B$  is permanently zero. On the other hand, in figure 3(c) we shine the  $\pi$ -pulse gaussian-shaped LP laser pulse with the amplitude 2.5 GV/m and pulse duration 38 fs. Similarly to Fig. 3(b), the polarization direction is in-phase direction to excite to quasi-degenerate electronic excited states  $a$  and  $b_1$ .  $J_L$  and  $J_R$  oscillate in the opposite phase, and as a characteristic feature  $J_B$  is generated, and the amplitude of transferred current

is smaller than the amplitudes of ring currents. Transfer of ring currents will occur if the created coherent excited states belong to different irreducible representations A and B.

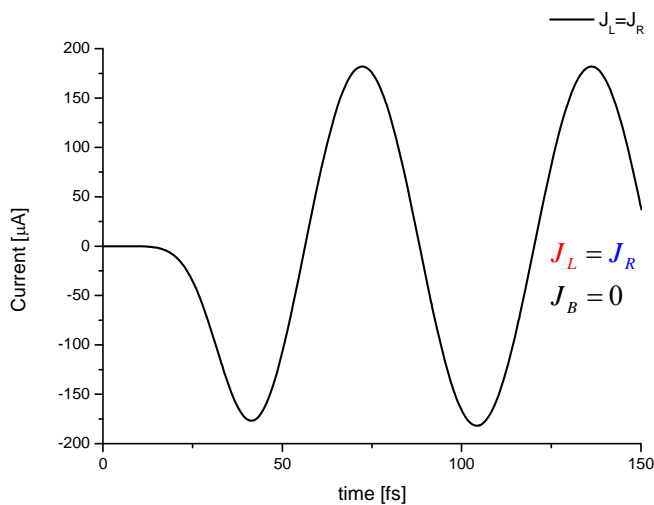
A three-dimensional plot of the resultant angular momentum switching based on the sequential four-step scheme is seen in Fig. 4. It can be seen from Fig. 4a that the angular momenta were successfully controlled by the pulses depicted in Fig. 4b, i.e., both the rotational axis (parallel to the Z or X axis) and the rotational direction around the axis (clockwise or anticlockwise) were satisfactorily controlled by the sequential four-step process. In Fig. 4b, the quantum control at each switching step was carried out by using overlapped pump and dump pulses with specific polarization directions.

For the present effective ultrafast quantum switching, overlap between the pump and dump pulses is essential: the resultant electric field is rotated as an elliptically polarized one in the overlapped region, and the electric field forces the rotating  $\pi$  electrons to induce the reverse rotation that occurs in this overlapped region. As a result, the electronic angular momentum or coherence between two electronic quasi-degenerate states is erased.

(a)



(b)



(c)

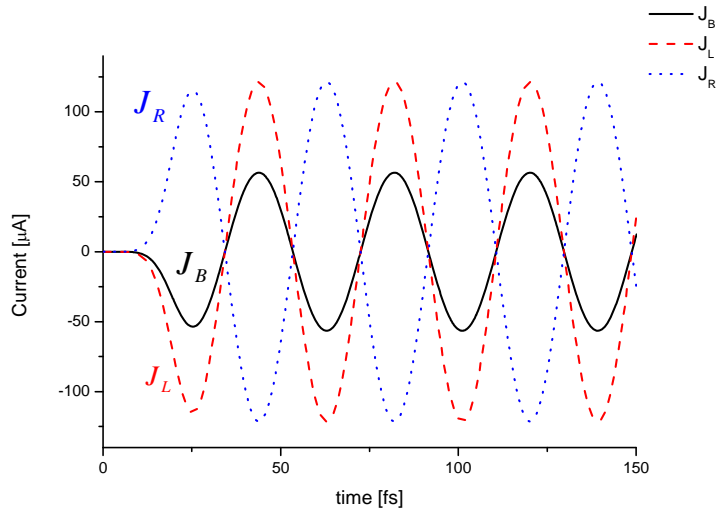


Fig. 3. (a) Definitions of directions of the ring current  $J_L$  ( $J_R$ ) on  $L$  ( $R$ ) phenol ring, and the bridge bond current  $J_B$  are given. (b) Time evolution of ring currents  $J_L$ ,  $J_R$  and bridge bond current  $J_B$  are plotted. Here coherent electronic excited states  $b_1$  and  $b_2$  are created with in-phase relative coherence by a LP laser pulse with the amplitude 1.2 GV/m and pulse duration 64 fs. (c) Time evolution of ring currents  $J_L$ ,  $J_R$  and bridge bond current  $J_B$  are plotted. Here coherent electronic excited states  $a$  and  $b_1$  are created with in-phase relative coherence by a LP laser pulse with the amplitude 2.5 GV/m and pulse duration 38 fs.

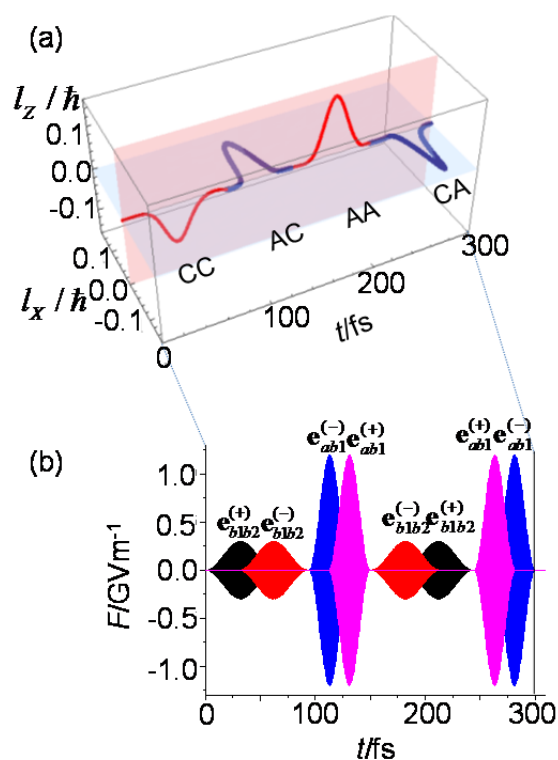


Fig. 4. (a) Sequential four-step switching of  $\pi$ -electron rotations in (*P*)-2,2'-biphenol. (b) Electric fields of the sequence of overlapped pump and dump pulses.

## 5. Summary and conclusions

In conclusion we have calculated a coherent  $\pi$  electron angular momentum and ring current in chiral molecule, (*P*)-2,2'-biphenol by using the UV linearly polarized laser pulse. We showed time-dependent coherent ring currents and angular momentum for three types of in-phase electronic coherent excited states  $(a+b_1)$ ,  $(a+b_2)$  with B symmetry and  $(b_1+b_2)$  with A symmetry in the point group  $C_2$ . As a characteristic feature for electronic coherent states  $(a+b_1)$  and  $(a+b_2)$ , a non-zero bridge bond current appears and oscillates between two phenol rings, while for electronic coherence  $(b_1+b_2)$  the bridge bond current disappears permanently. The direction of resultant angular momentum for electronic coherences  $(a+b_1)$  and  $(a+b_2)$  is parallel to Z-axis, while for electronic coherence  $(b_1+b_2)$  is parallel to X-axis. The initial directions of ring currents and angular momenta are determined from the initial phases of electronic coherences.

As an example of ultrafast quantum switching we have demonstrated an ultrafast two-dimensional switching of  $\pi$ -electron angular momentum in (*P*)-2,2'-biphenol using a sequence of overlapped pump-dump pulses with different phase and polarization direction. The key points for the multi-dimensional quantum switching is to coherently excite quasi-degenerate electronic states of a nonplanar chiral aromatic ring molecules with covalently bonded aromatic rings. Finally it would be fascinating to show methods of directly measuring the coherent electronic dynamics of a nonplanar chiral aromatic molecule.

## Acknowledgement



This work was supported by the National Science Council of Taiwan (Grant No. 102-2112-M-001-003-MY3). H.M. would like to thank Professor J.-L. Kuo for his critical comments and support.

### References

- [1] F. Remacle and R. D. Levine, *Phys. Rev. A* **83**, 013411 (2011).
- [2] I. S. Ulusoy and M. Nest, *J. Am. Chem. Soc.* **133**, 20230 (2011).
- [3] Y. Fujimura and H. Sakai, *Electronic and Nuclear Dynamics in Molecular Systems* (World Scientific, Singapore, 2011), p. 117.
- [4] F. Krausz and M. Ivanov, *Rev. Mod. Phys.* **81**, 163 (2009).
- [5] M. Nest, F. Remacle, and R. D. Levine, *New J. Phys.* **10**, 025019 (2008).
- [6] F. Remacle, M. Nest, and R. D. Levine, *Phys. Rev. Lett.* **99**, 183902 (2007).
- [7] P. Krause, T. Klamroth, and P. Saalfrank, *J. Chem. Phys.* **123**, 074105 (2005).
- [8] P. Kral, T. Seideman, *J. Chem. Phys.* **123**, 184702 (2005).
- [9] I. Barth and J. Manz, *Angew. Chem., Int. Ed.* **45**, 2962 (2006).
- [10] I. Barth, J. Manz, Y. Shigeta, and K. Yagi, *J. Am. Chem. Soc.* **128**, 7043 (2006).
- [11] M. Kanno, H. Kono, and Y. Fujimura, *Angew. Chem., Int. Ed.* **45**, 7995 (2006).
- [12] M. Kanno, K. Hoki, H. Kono, and Y. Fujimura, *J. Chem. Phys.* **127**, 204314 (2007).
- [13] H. Mineo, Y. Teranishi, M. Yamaki, M. Hayashi, S.H. Lin, and Y. Fujimura, *J. Am. Chem. Soc.* **134**, 14279 (2012).
- [14] H. Mineo, S.H. Lin, and Y. Fujimura, *J. Chem. Phys.* **138**, 074304 (2013).